BULLETIN OF THE POLISH ACADEMY OF SCIENCES
TECHNICAL SCIENCES
Vol. 58, No. 1, 2010

Cross-polarized normal mode patterns at a dielectric interface

W. NASALSKI*

Institute of Fundamental Technological Research, Polish Academy of Sciences, 5B Pawińskiego St., 02-106 Warsaw, Poland

Abstract. Basic features of narrow optical beam interactions with a dielectric interface are analysed. As it was recently shown, two types of paraxial beams – elegant Hermite-Gaussians of linear polarization and elegant Laguerre-Gaussians of circular polarization – can be treated as vector normal modes of the interface [1]. In this contribution the problem of normal modes is discussed with special attention paid for the case of beam oblique incidence. Excitation of higher-order modes by cross-polarization coupling is described and it is shown that this process critically depends on a propagation direction of the incident beam. Besides the expected changes of mode indices induced by generalised transmission and reflection matrices, the new phenomenon of optical vortex spectral splitting at the interface is revealed and off-axis spectral placements of the splitted vortices are determined. Results of numerical simulations given here for beam reflection entirely confirm theoretical predictions even for beams beyond the range of paraxial approximation.

Key words: reflection, refraction, normal modes, elegant beams, Hermite-Gaussian beams, Laguerre-Gaussian beams, cross-polarization coupling, vortex excitation, vortex splitting, total internal reflection.

1. Introduction

A field structure of a bounded beam of light reflected or refracted at a planar interface differs from that of an incident beam in its polarization, intensity and phase distribution. It is known that a cross-polarization coupling (XPC) of mutually orthogonal beam components is responsible for these differences [1], in spite of the direct beam amplitude reduction determined by the Fresnel coefficients [2]. The field distribution of the reflected or refracted beam component of one – from the two orthogonal – polarization basically mimics the field distribution of the incident beam. However, in the opposite beam component, the XPC effect leads to the excitation of higher-order or lower-order beam modes. This process critically depends on polarization and a propagation direction of the incident beam. Details of analysis of these phenomena were presented in [1], where also normal modes of the interface were defined. Although those definitions are almost obvious for normal incidence of paraxial beams, the case of beam oblique incidence needs more careful examination. This paper is mainly devoted to this problem.

It is also well understood that a field structure of bounded beams of light reflected or refracted at a planar interface differs from that prescribed by geometrical optics (g-o) not only in its polarization, intensity and phase transverse distribution but also by positions and directions of their beam axes [3, 4]. For sufficiently wide beams these differences can be described approximately by the beam frame spatial displacements from g-o predictions and by appropriate coordinate scaling (see e.g. [4] and references therein). Within effects of this sort the most known are the longitudinal Goos-Hänchen (G-H) [5, 6] and transverse Imbert-Fedorov (I-F) [7, 8] shifts or displacements. However, this geometrical approach works well for three-dimensional (3D) beams of cross-section diameters not less than around ten wavelengths. Moreover, even in this range and in spite of the case of the fundamental Gaussian, only higher-order non-singular beams like Hermite-Gaussian (HG) beams, the beams the field of which can be factorised into two two-dimensional (2D) beam fields, can be in principle treated efficiently in this way [4]. For these reasons the approximations of this sort do not seem suitable for the general analysis of the XPC beam-interface interactions.

Recently, beams of helical phase structure like Laguerre-Gaussian (LG) beams have been under intense research, because of many interesting applications ranging from classical to quantum optics, including those in nanophotonics, nanomaterial modelling, optical informatics as well as optical communication and visualisation in biology and medicine. However, the narrow LG beams suffer from such huge distortions during their reflection/transmission at the interface [9] that their description only in terms of the spatial shifts may appear insufficient even approximately. In other words, the field distribution of the LG beams in their amplitude and phase is rather distorted than displaced at the interface, especially in the case of critical incidence. It seems that reasons for these distortions are inhibited, besides of beam elliptic polarization, in the very specific interrelations between beam angular momentum, beam spectrum and placement of optical vortices embedded in the beam field [10]. A remedy in this situation may be to search for the information on beams directly in their field distribution exactly evaluated in the spectral domain [11], instead of approximate estimation of their field distribution by the spatial beam shifts. Within this approach the G-H and I-F spatial shifts are replaced by their phase counterparts in the spectral domain what makes the analysis in principle exact and leads to a form of the field patterns suitable for their immediate interpretation. Therefore, the spectral, instead of the spatial, approach removes the issue of the beam

*e-mail: wnasal@ippt.gov.pl

spatial shifts from theoretical considerations presented in this work.

Exactly this type of spectral analysis of vector beam fields at the dielectric interface was presented in [1]. The HG and LG beams in their elegant version, devised some time ago by Siegman [12, 13], served as a starting point in this analysis. Such beams, with their definitions appropriately modified and their possible non-paraxial extensions, appeared to be good candidates for normal modes at any planar dielectric structure. It was shown that the XPC effect is responsible for excitation of higher-order beams at such a structure. Although the method presented in [1] is quite general, this contribution extends further those results. The beam reflection for arbitrary beam incidence direction will be discussed here in parallel in the configuration and spectral domains. Similarities and differences in behaviour of HG and LG beams at the interface will be considered, basic mechanism of optical vortices excitation and splitting will be described in detail and off-axis placements of excited optical vortices will be determined in the beam spectra. Numerical examples, showing reflection of the beams with their radius of the order of one wavelength, that is narrow enough to be below the paraxial limit, will be presented. The interface will be considered as homogeneous, lossless and isotropic. Only numerical results on beam internal reflection at the interface, with a dielectric contrast equal to 2, will be given, as those on beam refraction were already reported in [1].

In Sec. 2 basic relations pertaining elegant beams will be shortly outlined and their modifications yielding the definitions of the normal modes at the interface will be defined. Section 3 and 4 are devoted to the HG and LG modes, respectively, where theoretical predictions will be presented and verified by numerical simulations. Only basic expressions necessary to interpret the XPC phenomenon under beam transmission and reflection will be given. Details of their derivation were presented in [1], which in turn follows earlier author's analyses [14–16] published in the past in another context. Note that the idea of the XPC beam-interface interactions was first explicitly introduced in [15] and subsequently applied in evaluation of field distribution of the first-order [17] or all higher-order [18] modes excited by the XPC effects at the interface. Finally, main conclusions summarise the paper in Sec. 5. In addition, definitions of generalized transmission and reflection coefficients will be given in Appendix 1 and the issue of the beam shifts will be briefly commented in Appendix 2.

2. Basic definitions for elegant beams

There are two levels of spectral analysis of beam fields at the interface. At the geometric-optical (g-o) level the standard Snell and Fresnel laws govern a single plane wave incident at a polar incidence angle $\vartheta^{(i)}$. On the second level plane waves are spectral ingredients of the 3D beams and therefore dependent, besides $\vartheta^{(i)}$, on an azimuthal incidence angle φ. In this paper the beams are treated analytically and exactly on the second level, where the well-known Fresnel coefficients should be replaced in the spectral or momentum domain by appropriately defined transmission and reflection matrices, dependent on both angles $\vartheta^{(i)}$ and φ. Subsequently, by the use of the standard 2D Fourier transform, the beam fields are obtained numerically in the configuration or direct domain, with incidence angles $\theta^{(i)}$ and ψ (see Fig. 1).

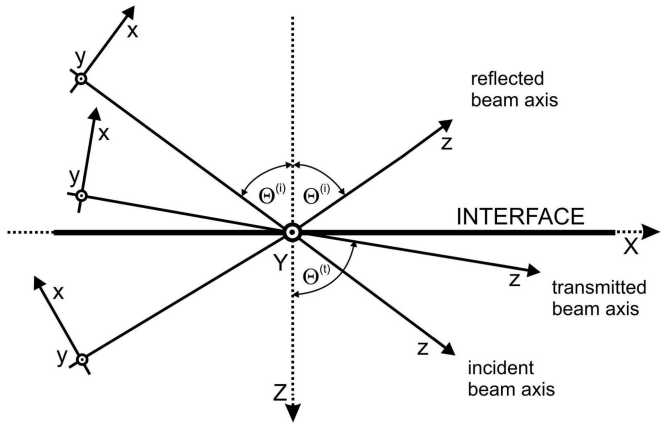

Fig. 1. Interface $OXYZ$ and beam $Oxyz$ reference frames viewed in a main incidence plane $X-Z$; local planes of incidence are given by rotation of the plane $X-Z$ by an azimuthal angle ψ around the axis Z. Beam waist centres are placed in centres of beam frames, incidence of internal reflection is assumed.

In general, a complex electric field vector $\underline{E}_{\perp}^{(b)}$ transverse to the normal to the interface is obtained by the decomposition consisted of *suitably defined* mode solutions $\underline{G}_{c,d}^{(b)}$ to the problem:

$$\underline{E}_{\perp}^{(b)}(X,Y,Z) = \sum_{c,d} a_{c,d}^{(b)}\, \underline{e} \circ\ \underline{G}_{c,d}^{(b)}(X,Y,Z'), \qquad (1)$$

where $a_{c,d}^{(b)}$ are expansion coefficients, c and d are expansion indices, $Z' = Z - Z_w$, as the beam waist centres are assumed to be placed in general in planes $Z = Z_w$ parallel to the interface, $b = i, t, r$ indicate the incident, transmitted (refracted) and reflected beam, respectively (see Fig. 1). The polarization 2D versor $\underline{e}$ is defined in the interface plane $X - Y$. Only monochromatic fields are considered with the propagation term $\exp(-i\omega t + \mathrm{ik}^{(b)} Z' / \cos\theta^{(b)})$ assumed and suppressed in all field expressions, where ω is an angular frequency and $k^{(b)}$ are wave numbers of the respective beam fields with their Z components fixed by the divergence constraint. Note that in the following the alternative notation $k^{(i)} = k^{(r)} \equiv k$ also will be used.

For uniform beam polarization a scalar wave approach suffices to describe the beam field in its paraxial region with polarization components of $\underline{G}_{c,d}^{(b)}$ regarded as modes of the optical system. However, the true modes at the interface are vectors not scalars because the interface couples the polarization and spatial characteristics of beam fields [1]. Therefore, the scalar modes are considered in this Section, their vector counterparts will be analysed in the next Sections. The aim of this paper is to show and discuss examples of these *suitably defined* partial solutions to the problem. If the modes consti-

tute a complete and orthogonal or bi-orthogonal set of square integrable functions, they can be called as *normal modes* of the interface.

For any normal mode $\underline{G}_{c,d}^{(b)}$ the expansion (1) resolves into only one term representing the field $\underline{E}_{\perp}^{(b)}$ of all three beams $b = i, t, r$, with the scalar modes attributed to each polarization component of these beams. Two sets of such beams will be considered in this Section within the paraxial approximation – elegant Hermite-Gaussian (EHG) beams and elegant Laguerre-Gaussian (ELG) beams [12, 13, 19, 20], as the grounds on which the vector modes of the interface can be build. They specify solutions to the problem in the two coordinate systems: Cartesian $OXYZ$ of rectangular symmetry and cylindrical $Or_{\perp}\psi Z$ of cylindrical symmetry. It appears that the elegant beams with their possible non-paraxial extensions are particularly suitable in description of beam fields at the interface provided that they are defined at the interface plane $X - Y$ instead, as usual, in the beam transverse plane $x - y$ (see Fig. 1) [1].

Let us consider *normal incidence of paraxial beams* first. In this case the two planes $X - Y$ and $x - y$ coincide. In the Cartesian coordinates the Fock (paraxial) wave equation reads

$$\left\{ ik^{(b)}\partial_Z + \frac{1}{2}(\partial_X^2 + \partial_Y^2) \right\} G_{m,n}^{(EH)}(X, Y, Z') = 0, \qquad (2)$$

with the elegant solution in the form of the EHG beam mode $G_{m,n}^{(EH)}$ specified by the X and Y indices given by two integers m and n, respectively, their order $N^{(EH)} = m + n$ and the beam waist placement in the plane $Z = Z_w$ [1, 20]:

$$G_{m,n}^{(EH)}(X, Y, Z') = (w_w)^{m+n}\partial_X^m\partial_Y^n\, G_{0,0}^{(EH)}(X, Y, Z'). \quad (3)$$

$$\begin{aligned} &G_{0,0}^{(EH)}(X, Y, Z') = \\ &= (w_w/v(Z'))^2 \exp\left(-(1/2)(X^2 + Y^2)/v^2(Z')\right), \end{aligned} \qquad (4a)$$

where, $z_D = kw_w^2$ is the diffraction length or Rayleigh range, w_w and $v(Z') = w_w(1 + iZ'/z_D)^{1/2}$ are the waist and complex radii of the fundamental Gaussian mode $G^{(EH)}$, respectively. The Gaussian mode is assumed in this work as symmetric with circular cross-section, i.e. with the same waist radii $w_{wX} = w_{wY} = w_w$ in X and Y directions, in the plane $Z' = 0$. For elliptic cross-section of the beam modifications are straightforward. The EHG functions $G_{m,n}^{(EH)}$ are expressed by the Hermite polynomials $H_m(x)$ of order m:

$$\begin{aligned} &G_{m,n}^{(EH)}(X, Y, Z') = (-w_w)^{m+n} \\ &H_m(2^{-1/2}X/v(Z'))H_n(2^{-1/2}Y/v(Z'))G_{0,0}^{(EH)}(X, Y, Z'). \end{aligned} \qquad (5)$$

The amplitude of the EHG beam is determined here by the condition $G^{(EH)}(0, 0, 0) = 1$.

Similar definitions can be applied in the complex coordinates specific to systems of cylindrical symmetry: $\varsigma = 2^{-1/2}(X + iY)$ and its complex conjugate $\overline{\varsigma}$. Then the paraxial wave equation reads [1, 20]:

$$\left\{ ik^{(b)}\partial_Z + \partial_\varsigma\partial_{\overline{\varsigma}} \right\} G_{p,l}^{(EL)}(\varsigma, \overline{\varsigma}, Z') = 0, \qquad (6)$$

with the elegant solution given in a form of ELG modes:

$$G_{p,l}^{(EL)}(\varsigma, \overline{\varsigma}, Z') = (w_w)^{2p+l}\partial_\varsigma^p\partial_{\overline{\varsigma}}^{p+l}G_{0,0}^{(EL)}(\varsigma, \overline{\varsigma}, Z'), \qquad (7)$$

$$G_{0,0}^{(E,L)}(\varsigma, \overline{\varsigma}, Z') = (w_w/v(Z'))^2 \exp\left(-\varsigma\overline{\varsigma}v^{-2}(Z')\right), \quad (8a)$$

of the radial p and azimuthal l indices contributing to the beam order $N^{(EL)} = 2p + l$. Note that the fundamental Gaussian $G_{0,0}^{(EH)}(X, Y, Z')$ is equal to $G_{0,0}^{(EL)}(\varsigma, \overline{\varsigma}, Z')$ for $X = 2^{-1/2}(\varsigma + \overline{\varsigma})$ and $Y = -i2^{-1/2}(\varsigma - \overline{\varsigma})$. The ELG modes are expressed by the associated Laguerre polynomials $L_p^l(x)$:

$$\begin{aligned} G_{p,l}^{(EL)}(\varsigma, \overline{\varsigma}, Z') &= (-1)^{p+l}(\varsigma_\perp/v)^l(v/w_w)^{-(2p+l)} \\ &\times p!L_p^l(\varsigma_\perp^2/v^2)G_{0,0}^{(EL)}(\varsigma, \overline{\varsigma}, Z')\exp(il\psi), \end{aligned} \qquad (9)$$

where $\varsigma = \varsigma_\perp \exp(i\psi)$. The azimuthal index or winding number l is any integer number associated with the Z component of the orbital angular momentum carried by the ELG beam. When $l \neq 0$ it is equal to a topological charge of an optical vortex of the LG beam. The radial index or node number p is a nonnegative integer, which determines a radially symmetric beam structure with, besides the fundamental Gaussian case, zero on-axis intensity. Note that also the closed form non-paraxial extension of the paraxial formalism for the elegant beams was published very recently [21].

For *oblique incidence* the above definitions of the paraxial elegant beams are exactly valid after the replacement of the "interface" coordinates X, Y and Z by the coordinates x, y and z belonging to the beam frame (cf. Fig. 1). However, such the replacement does not lead to the definition of the beam modes at the interface, for which the condition – for one incident mode only one reflected mode and one transmitted mode of the same type are excited in each field component – should be exactly fulfilled. In other words, the common definitions (given in the beam frame $Oxyz$) of the elegant beams do not fit, in the case of oblique incidence, to the action of the interface on these beams (as described later in the X and Y coordinates).

The functional form of the beam modes for oblique incidence is determined here by the form of the transmission and reflection matrices given in the next two Sections. The fundamental Gaussian beam fields are defined, as usual, in the beam coordinate frames $Oxyz'$ and $O\xi\overline{\xi}z'$, where $z' = Z'/\cos\theta^{(i)}$ and $\xi = 2^{-1/2}(x + iy)$:

$$\begin{aligned} &G_{0,0}^{(EH)}(X, Y, Z') = \\ &= (w_w/v(z'))^2 \exp\left(-(1/2)(x^2 + y^2)/v^2(z')\right), \end{aligned} \qquad (4b)$$

$$\begin{aligned} &G_{0,0}^{(EL)}(\varsigma, \overline{\varsigma}, Z') = \\ &= (w_w/v(z')/v(z'))^2 \exp\left(-\xi\overline{\xi}v^{-2}(z')\right). \end{aligned} \qquad (8b)$$

In these equations the interface coordinates X and Z', and consequently also ς and $\overline{\varsigma}$, are obtained from the beam coordinates x and z', by their rotation about Y axis through the incident angle $\theta^{(i)} \neq 0$, which also affects ξ and $\overline{\xi}$. In effect, for example, the beam circular cross-section commonly defined in the beam transverse plane $z' = const.$ resolves in

Eqs. (4b) and (8b) into the beam elliptic cross-section in the interface plane $Z' = const.$ and vice versa. The fundamental Gaussians (4b) and (8b) serve now for the determination of the higher-order mode fields $G_{m,n}^{(EH)}$ and $G_{p,l}^{(EL)}$ at the interface by using Eqs. (3) and (7) of the same form as for the normal incidence.

Moreover, all these beam fields acquire at the plane $Z' = const.$ the additional phase shift $\Phi(X) = k^{(i)} X \sin\theta^{(i)}$ as the result of the tilted beam phase fronts with respect to the interface plane:

$$G_{m,n}^{(EH)}(X,Y,Z') \rightarrow G_{m,n}^{(EH)}(X,Y,Z') \exp(ik^{(i)} X \sin\theta^{(i)}), \tag{10}$$

$$G_{p,l}^{(EL)}(\varsigma,\overline{\varsigma},Z') \rightarrow \rightarrow G_{p,l}^{(EL)}(\varsigma,\overline{\varsigma},Z') \exp(ik^{(i)} 2^{-1/2}(\varsigma+\overline{\varsigma})\sin\theta^{(i)}). \tag{11}$$

Therefore, in the paraxial range and for $m = 0 = n$ or $p = 0 = l$ (no differentiation), the normal modes such defined are just the common fundamental Gaussians. The higher-order normal modes defined here by Eqs. (3) and (7) differ for oblique incidence, however, from the common elegant modes, as defined e.g. in [13, 20]. The difference consists of the replacement in those definitions of the beam frame derivatives ∂_x and ∂_y or ∂_ξ and $\partial_{\overline{\xi}}$ in the plane $z' = const.$ by the interface frame derivatives ∂_X and ∂_Y or ∂_ς and $\partial_{\overline{\varsigma}}$ in the plane $Z' = const.$

The beam fields such defined obey the Helmholtz (reduced wave) equation in the coordinates X, Y and Z, instead of the paraxial one in the coordinates x, y and z, and they should be in general understood as the non-paraxial beam fields. They will be called here as the projected elegant – PEHG and PELG – beams consistently with their definitions given above for oblique incidence. More specifically, all the beams considered in this analysis, normal or oblique to the interface, are treated as non-paraxial – note that in all numerical simulations a cross-sectional radius of the beams will be taken as corresponding to $kw_w = 2\pi$, that is below the paraxial limit.

Therefore, the beam fields considered here satisfy in general the full set of Maxwell equations for an arbitrary value of Z, together with the field continuity relations at the interface plane $Z = 0$. However, all analytical field expressions defined by the definitions (3), (7), (10) and (1) are necessary and are given here only in a single plane – the interface plane. Next, starting from the field distribution obtained by the use of these equations in the interface plane, one can rebuild the normal mode field distribution in the vicinity of the interface plane for $Z \neq 0$, on the grounds of a full set of Maxwell equations. But evaluation of the beam field outside the interface plane is not necessary in this analysis and remains out of the scope of this paper.

3. Beam-interface relations in rectangular coordinates

Let us start from the Fresnel transmission and reflection coefficients t_p, r_p and t_s, r_s for a single plane wave of an arbitrary polarization parameter $\widetilde{\chi}_{(p,s)}^{(i)} = \widetilde{E}_p^{(i)} / \widetilde{E}_s^{(i)}$ specified by its p and s polarization components $\widetilde{E}_p^{(i)}$ and $\widetilde{E}_s^{(i)}$, respectively. The plane wave is incident on the interface under the incidence angle $\vartheta^{(i)}$. In the linear TM/TE polarization basis $\underline{e}_{(X,Y)} = [\underline{e}_X, \underline{e}_Y]$ these coefficients defined in the interface plane $X - Y$ yield diagonal elements of the Fresnel transmission and reflection matrices $\underline{\underline{t}}_{(p,s)}$ and $\underline{\underline{r}}_{(p,s)}$: ηt_p, r_p for TM beam component and t_s, r_s for TE beam component, respectively, where $\eta = \cos\vartheta^{(t)} / \cos\vartheta^{(i)}$. Further it is stipulated that $r_p = r_s = 1$ for critical incidence of total internal reflection (TIR). Then, the continuity relations of tangent field components in the interface plane are given by $\underline{\underline{t}}_{(p,s)} = \underline{\underline{1}} + \underline{\underline{\sigma}}\,\underline{\underline{r}}_{(p,s)}$, where $\underline{\underline{1}}$ is a unit matrix and $\underline{\underline{\sigma}}$ stand for diagonal Pauli matrix of $\sigma_{XX} = -1 = -\sigma_{YY}$. Note that the Fresnel matrices do not depend of the azimuthal angle φ and are defined in one, usually taken as a main, incidence plane [14].

However, 3D beams are composed of infinite number of plane waves and each plane wave is distinguished by two angles of incidence – a polar angle ϑ and an azimuthal angle φ, where the latter defines a local incidence plane attributed to this plane wave [14]. The matrices $\underline{\underline{t}}_{(p,s)}$ and $\underline{\underline{r}}_{(p,s)}$ are then should be replaced by the matrices $\underline{\underline{t}}_{(X,Y)}$ and $\underline{\underline{r}}_{(-X,Y)}$, which relate spectral components $\underline{\widetilde{E}}_{(X,Y)}^{(b)} = [\widetilde{E}_X^{(b)},\ \widetilde{E}_Y^{(b)}]^T$, $b = i, t$ and $\underline{\widetilde{E}}_{(-X,Y)}^{(r)} = [-\widetilde{E}_X^{(r)},\ \widetilde{E}_Y^{(r)}]^T$ of the beam fields at the interface [16]:

$$\underline{\widetilde{E}}_{(X,Y)}^{(t)} = \underline{\underline{t}}_{(X,Y)} \underline{\widetilde{E}}_{(X,Y)}^{(i)}, \qquad \underline{\widetilde{E}}_{(-X,Y)}^{(r)} = \underline{\underline{r}}_{(-X,Y)} \underline{\widetilde{E}}_{(X,Y)}^{(i)}, \tag{12}$$

$$\underline{\underline{t}}_{(X,Y)} = \underline{\underline{t}}_{(p,s)} + t_{CX} \begin{bmatrix} 0 & 1 \\ 1 & 0 \end{bmatrix} \sin 2\varphi + + 2t_{CX} \begin{bmatrix} -1 & 0 \\ 0 & 1 \end{bmatrix} \sin^2\varphi, \tag{13}$$

$$\underline{\underline{r}}_{(-X,Y)} = \underline{\underline{r}}_{(p,s)} + r_{CX} \begin{bmatrix} 0 & 1 \\ -1 & 0 \end{bmatrix} \sin 2\varphi - - 2r_{CX} \begin{bmatrix} 1 & 0 \\ 0 & 1 \end{bmatrix} \sin^2\varphi, \tag{14}$$

$$t_{CX} = \frac{1}{2}(\eta t_p - t_s) = -\frac{1}{2}(r_p + r_s) = -r_{CX}, \tag{15}$$

where t_{CX} and r_{CX} are the XPC coefficients. Their role in the XPC interactions will appear evident further. The matrices $\underline{\underline{t}}_{(X,Y)}$ and $\underline{\underline{r}}_{(-X,Y)}$ fulfil there the field continuity relation $\underline{\underline{t}}_{(X,Y)} = \underline{\underline{1}} + \underline{\underline{\sigma}}\,\underline{\underline{r}}_{(-X,Y)}$ at the interface and are dependent this time not only on the incidence angle $\vartheta^{(i)}$ but also on the azimuthal angle $\varphi = \arctan(k_Y / k_X)$. Note that because $\cos 2\varphi = (k_X^2 - k_Y^2) k_\perp^{-2}$ and $\sin 2\varphi = 2k_X k_Y k_\perp^{-2}$, where $\underline{k} = [\underline{k}_\perp, k_Z^{(b)}]^T$, $\underline{k}_\perp = [k_X, k_Y]^T$ and $k_Z^{(t)} = \eta k_Z^{(i)} = \eta k_Z^{(r)}$,

the matrices (13)–(14) are equivalent to those given in a different form by in [1], where it was also shown that the matrices (13)–(14) become diagonal by introduction the "linear" polarization parameter $\widetilde{\chi}^{(i)}_{(X,Y)} = \widetilde{E}^{(i)}_X / \widetilde{E}^{(i)}_Y$ of the incident beam [1]. Then the TM and TE generalized 3D-counterparts t_{TM}, r_{TM}, t_{TE} and r_{TE} of the Fresnel coefficients [15] can be extracted form these matrices (see Appendix I).

Although these matrices are exact, the subsequent terms in their decomposition can be interpreted as the zero-order (Fresnel), first-order and second-order (with respect to k_Y or φ) contributions to beam transmission and reflection. Only the first-order terms are created by the XPC effect at the interface and only these terms are dependent – through the polarization parameter $\widetilde{\chi}^{(i)}_{(X,Y)}$ – on a polarization state of the incident beam field. Certainly, besides the azimuthal angle φ the matrices (13)–(14) depend also, through the Fresnel coefficients, on the polar angle $\vartheta^{(i)}$. Exactly in the incidence plane ($\varphi = 0$) the first-order and second-order terms in Eqs. (13)–(14) disappear and only the zero-order term, determined by rules of geometrical optics, remains. In this plane the generalised matrices (13)–(14) resolve plainly into the Fresnel or g-o matrices. As the Fresnel matrices are diagonal in the Cartesian coordinates the g-o approach to the problem disregards the XPC effects in the beam-interface interactions.

The transmission and reflection matrices (13)–(14) show distinct symmetry with respect to the incidence ($Y = 0$) and transverse ($X = 0$) planes and their action is particularly specific in the case of incident beams possessing the same type of symmetry. Within this class of beams the EHG/PEHG beams of TM or TE linear polarization are of particular importance. In the spectral domain their definition (3)–(4) yields for normal incidence:

$$\begin{aligned} &\widetilde{G}^{(EH)}_{m,n}(k_X, k_Y, Z') = \\ &= (iw_w)^{m+n} k_X^m k_Y^n \widetilde{G}^{(EH)}_{0,0}(k_X, k_Y, Z'), \end{aligned} \tag{16}$$

where $\widetilde{G}^{(EH)}_{0,0} = 2\pi \exp\left[-(1/2)k_\perp^2 v^2\right]$ and $\widetilde{G}^{(EH)}_{m,n}$ mean a 2D Fourier transform of $G^{(EH)}_{m,n}$. Let us first consider normal incidence of the beam $\underline{\widetilde{E}}^{(i)} = [\widetilde{a}_X, \widetilde{a}_Y]^T \widetilde{G}^{(EH)}_{m,n}$ of the EHG mode shape and of arbitrary polarization $\widetilde{\chi}^{(i)}_{(X,Y)} = \widetilde{a}_X / \widetilde{a}_Y$ specified by the beam components $\widetilde{a}_X$ and $\widetilde{a}_Y$, in general complex and dependent on k_X and k_Y in the case of non-uniform polarization. We assume that the impact of the second-order term in the decomposition (13)–(14) is negligibly small, as previous numerical simulations confirm this assumption [1]. Then, within this first-order approximation and using the substitution $\sin 2\varphi = 2k_X k_Y k_\perp^{-2}$, Eqs. (12)–(16) yield the transmitted and reflected beam fields of the form [1]:

$$\begin{aligned} \begin{bmatrix} \widetilde{E}^{(t)}_X \\ \widetilde{E}^{(t)}_Y \end{bmatrix} &\cong \begin{bmatrix} \eta t_p \widetilde{a}_X \\ t_s \widetilde{a}_Y \end{bmatrix} \widetilde{G}^{(EH)}_{m,n} - \\ &- 2t_{CX}(k_\perp w_w)^{-2} \begin{bmatrix} \widetilde{a}_Y \\ \widetilde{a}_X \end{bmatrix} \widetilde{G}^{(EH)}_{m',n+1}, \end{aligned} \tag{17}$$

$$\begin{aligned} \begin{bmatrix} -\widetilde{E}^{(r)}_X \\ \widetilde{E}^{(r)}_Y \end{bmatrix} &\cong \begin{bmatrix} r_p \widetilde{a}_X \\ r_s \widetilde{a}_Y \end{bmatrix} \widetilde{G}^{(EH)}_{m,n} - \\ &- 2r_{CX}(k_\perp w_w)^{-2} \begin{bmatrix} \widetilde{a}_Y \\ -\widetilde{a}_X \end{bmatrix} \widetilde{G}^{(EH)}_{m',n+1}. \end{aligned} \tag{18}$$

It appears that the beams behave differently depending on their incidence angle [22].

For normal incidence $m' = m + 1$. Both indices in the beam component of the same polarization as that of the incident beam remain unchanged ($m \to m$ and $n \to n$). However, the beam component of the opposite (orthogonal) polarization shows clearly the action of the XPC effect [1, 15]. Both indices in this component are increased by one ($m \to m+1$ and $n \to n+1$) and thus the incident beam order $N^{(HG)} = m+n$ is increased there by 2 ($N^{(HG)} \to N^{(HG)} + 2$). Therefore, for incidence of EHG beams of a *single* TM or TE polarization component, the reflected beams are composed also of the EHG beams in the *two* TM and TE polarization components, with their indices exactly specified. The relations (17)–(18) are given in the spectral domain. The beam field distribution in the direct domain is obtained by the standard 2D Fourier transform of these relations.

For oblique incidence $m' = m$. The beam field definition (3) for EHG beam acquires the additional phase shift (10) what implies the spectral shift in the definition (16):

$$\begin{aligned} &\widetilde{G}^{(EH)}_{m,n}(k_X, k_Y, Z') \to \\ &\to \widetilde{G}^{(EH)}_{m,n}(k_X - k\sin\theta^{(i)}), k_Y, Z'). \end{aligned} \tag{19}$$

Moreover, the range of the azimuthal angle φ for significant spectrum amplitude contribution becomes so narrow [22] that this case is more appropriately described by applying the next step: $\sin 2\varphi \cong 2\sin\varphi = 2k_Y/k_\perp$ in the first-order approximation $\sin^2\varphi \cong 0$ to the exact expressions (13)–(14) of the transmission and reflection matrices (cf. Eq. (16) in [18]). By this additional approximation and with the replacement (19) the decomposition (17)–(18) still remains valid provided that now $m' = m$. Therefore, the PEHG beams under oblique incidence behave differently than the EHG beams under normal incidence. The beam modes are still of the incident beam shape for the same polarization component of the reflected beam. However, for the opposite field component only Y index is increased by one. In this beam component the mode indices (m, n) show transformation ($m \to m$ and $n \to n+1$) and the incident beam order $N^{(HG)} = m + n$ is increased only by one ($N^{(HG)} \to N^{(HG)} + 1$).

The EHG/PEHG beam field intensity spatial distribution at the interface is precisely confirmed in Figs. 2 and 3, where the first and the second rows pertain the beam field distribution in the configuration and spectral domains, respectively. Although the field decomposition (17)–(18) is only of the first-order, Figs. 2 and 3 indicate that this decomposition is still very accurate even for the beam waist radius of the order of one wavelength. For normal incidence of the EHG beam (cf. Fig. 2) the opposite polarization component of the reflected

beam acquires the new X and Y mode indices increased by 1 with respect to the incident beam mode. For oblique incidence of the PEHG beam (cf. Fig. 3), the X index change gradually diminishes with increasing incidence angle and a longitudinal spatial displacement of the whole field structure appears instead [18]. However, the issue of beam displacements is not discussed in this paper, although it may be essential in other applications of near field optics [23]. Note that due to the mirror symmetry in X and Y coordinates the deformations of the PEHG beams are not large and it is possible to describe them quantitatively also in the configuration domain, as outlined in Appendix 1. Note also that the (constant) spectral shift in Eq. (19) are removed from Figs. 2 and 3.

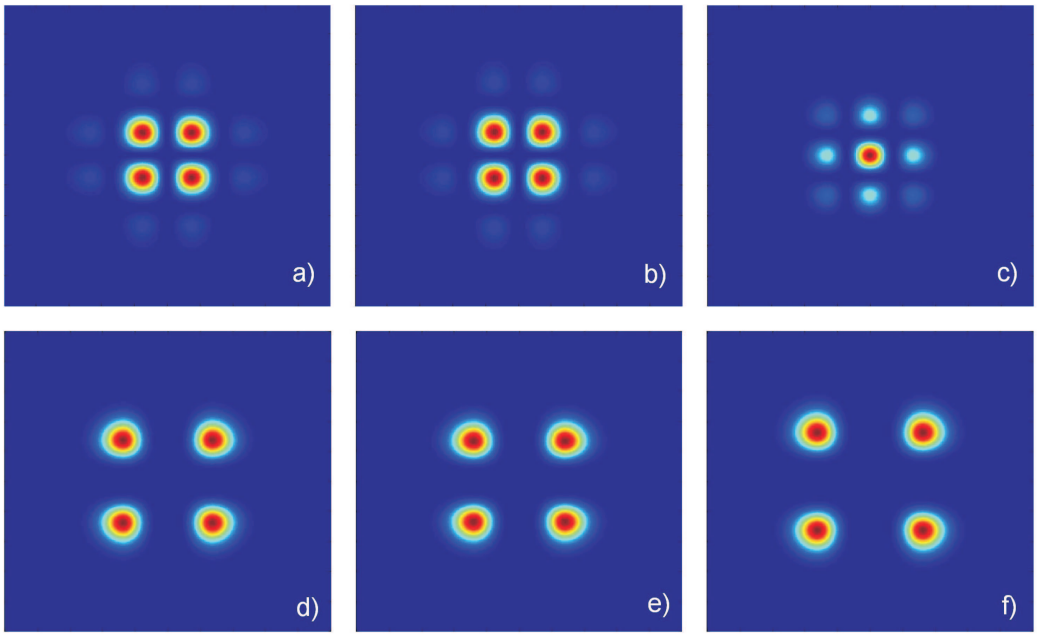

Fig. 2. Intensity transverse distribution of the EHG beam components evaluated in the interface plane; counterparts of the Figs. (a)–(c) in the configuration domain are depicted in the Figs. (d)–(f) in the spectral domain, respectively. The case of normal incidence ($\theta^{(i)} = 0^\circ$) of the collimated ($Z_w = 0$) beam is displayed at the interface for: (a) the incident beam of the $EHG_{3,3}$ pattern and of TE polarization, (b) the reflected beam TE component of the $EHG_{3,3}$ pattern, (c) the reflected beam TM component of the $EHG_{4,4}$ pattern (colour online)

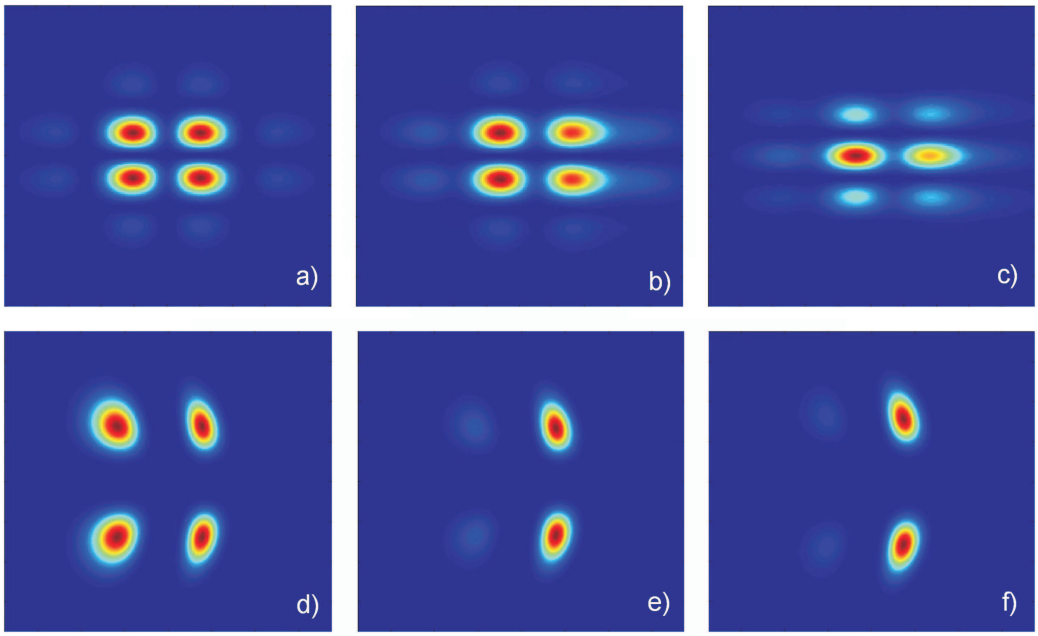

Fig. 3. Intensity transverse distribution of the EHG beam components evaluated in the interface plane; counterparts of the figures (a)–(c) in the spectral domain are depicted in the Figs. (d)–(f) in the spectral domain, respectively. The case of critical incidence ($\theta^{(i)} = 45^\circ$) of the beam collimated ($Z_w = 0$) is displayed at the interface for: (a) the incident beam of the $EHG_{3,3}$ pattern and of TE polarization, (b) the reflected beam TE component of the $EHG_{3,3}$ pattern, (c) the reflected beam TM component of the $EHG_{3,4}$ pattern (colour online)

4. Beam-interface relations in cylindrical coordinates

The EHG/PEHG beams are normal modes only within the first-order field approximation with respect to the azimuthal angle φ. The question therefore arises whether there are other beams with different shape and polarization, which can be considered as normal modes with their fields determined *exactly*. The answer is positive - the beams symmetric with respect to cylindrical coordinates of circular polarization are such good candidates in this case [1].

Therefore, let us now rewrite the expressions given previously for the EHG/PEHG beams through the straightforward unitary transformation in the circular CR/CL polarization basis $\underline{e}_{(R,L)}$, where the circular polarization means here the "interface" circular polarization defined in this plane. Thus, for oblique incidence, circular polarization commonly defined in the beam cross-section resolves into elliptic polarization in the interface plane and vice versa. Then the beam field vectors:

$$\underline{\widetilde{E}}^{(b)}_{(R,L)} = [\widetilde{E}^{(b)}_{R}, \widetilde{E}^{(b)}_{L}]^T = \\ = 2^{-1/2}\left[\widetilde{E}^{(b)}_{X} - i\widetilde{E}^{(b)}_{Y}, \widetilde{E}^{(b)}_{X} + i\widetilde{E}^{(b)}_{Y}\right]^T, \tag{20}$$

$$\underline{\widetilde{E}}^{(r)}_{(L,R)} = [\widetilde{E}^{(r)}_{L}, \widetilde{E}^{(r)}_{R}]^T = \\ = -2^{-1/2}\left[\widetilde{E}^{(r)}_{X} - i\widetilde{E}^{(r)}_{Y}, \widetilde{E}^{(r)}_{X} + i\widetilde{E}^{(r)}_{Y}\right]^T, \tag{21}$$

$b = i, t$ are interrelated at the interface by new transmission $\underline{\underline{t}}_{(R,L)}$ and reflection $\underline{\underline{r}}_{(L,R)}$ matrices [1, 18]:

$$\underline{\widetilde{E}}^{(t)}_{(R,L)} = \underline{\underline{t}}_{(R,L)}\underline{\widetilde{E}}^{(i)}_{(R,L)}, \\ \underline{\widetilde{E}}^{(r)}_{(L,R)} = \underline{\underline{r}}_{(L,R)}\underline{\widetilde{E}}^{(i)}_{(R,L)}, \tag{22}$$

$$\underline{\underline{t}}_{(R,L)} = \underline{\underline{t}}_{C} + \underline{\underline{t}}_{CX} = t_C \begin{bmatrix} 1 & 0 \\ 0 & 1 \end{bmatrix} + \\ + t_{CX} \begin{bmatrix} 0 & \exp(-2i\varphi) \\ \exp(+2i\varphi) & 0 \end{bmatrix}, \tag{23}$$

$$\underline{\underline{r}}_{(L,R)} = \underline{\underline{r}}_{C} + \underline{\underline{r}}_{CX} = r_C \begin{bmatrix} 1 & 0 \\ 0 & 1 \end{bmatrix} + \\ + r_{CX} \begin{bmatrix} 0 & \exp(-2i\varphi) \\ \exp(+2i\varphi) & 0 \end{bmatrix}, \tag{24}$$

$$t_C = \frac{1}{2}(\eta t_p + t_s), \qquad r_C = \frac{1}{2}(r_p - r_s) = 1 - t_C, \tag{25}$$

with the "circular" g-o coefficients t_C and r_C. The XPC coefficients t_{CX} and r_{CX} are defined earlier by Eq. (15). The field continuity relations at the interface now read $\underline{\underline{t}}_{C} = \underline{\underline{1}} - \underline{\underline{r}}_{C}$ and $\underline{\underline{t}}_{(R,L)} = \underline{\underline{1}} - \underline{\underline{r}}_{(L,R)}$ in the incidence plane ($\varphi = 0$) and in arbitrary ($\varphi = const.$) local plane, respectively. By introduction the "circular" polarization parameter $\widetilde{\chi}^{(i)}_{(R,L)} = \widetilde{E}^{(i)}_{R}/\widetilde{E}^{(i)}_{L}$ of the incident beam, the matrices (23)–(24) become diagonal. Then the CR and CL generalized 3D-counterparts t_{CR}, r_{CR}, t_{CL} and r_{CL} of the Fresnel coefficients can be extracted form these matrices (see Appendix 1).

For any polar angle $\vartheta^{(i)}$ and azimuthal angle φ the matrices $\underline{\underline{t}}_{(R,L)}$ and $\underline{\underline{r}}_{(L,R)}$ resolve into the diagonal matrices $\underline{\underline{t}}_{C}$ and $\underline{\underline{r}}_{C}$ determining the "direct" beam component of the same polarization as that of the incident beam and into the XPC antidiagonal matrices $\underline{\underline{t}}_{CX}$ and $\underline{\underline{r}}_{CX}$ determining the opposite beam component. Under beam transmission and reflection the related to them matrix elements $t_{CX}\exp(\pm 2i\varphi)$ and $r_{CX}\exp(\pm 2i\varphi)$ create, in the opposite beam components, additional vortices of the topological charge equal to ± 2. Positions of the excited vortices are determined by zeroes of the beam field and thus on zeroes of t_{CX} and r_{CX}. For normal incidence both types of vortices, these nested in the incident beam and these excited at the interface are placed in the centre of the coordinate system $k_X w_w = 0 = k_Y w_w$, that is exactly in the point where the spectrum of the incident higher-order ($|l| \geq 1$) is zero (see Eq. (28). Note that $t_{CX} = -r_{CX} = 0$ at this point. For oblique incidence, however, the spectrum centre acquires additional phase shift $2^{-1/2}k^{(i)}\sin\theta^{(i)}$ and the exited vortex is displaced additionally by the opposite spectral shift $-2^{-1//2}k^{(i)}\sin\theta^{(i)}$ to the position where again $t_{CX} = -r_{CX} = 0$. For critical incidence, for example, the displacement of the excited vortex induces the change from the point where $t_{CX} = -r_{CX} = -1$ to the point where $t_{CX} = -r_{CX} = 0$.

In the problem discussed here in the plane $k_X - k_Y$ no plane in general exists where the problem resolves into the standard Fresnel transmission or reflection and where the XPC effects disappears. In spite of this the matrices (23)–(24) can be also rewritten, similarly to the decomposition (13)–(14), into the zero-, first- and second- order terms with respect to φ:

$$\underline{\underline{t}}_{(R,L)} = \begin{bmatrix} t_C & t_{CX} \\ t_{CX} & t_C \end{bmatrix} + it_{CX}\begin{bmatrix} 0 & -1 \\ 1 & 0 \end{bmatrix}\sin 2\varphi - \\ - 2t_{CX}\begin{bmatrix} 0 & 1 \\ 1 & 0 \end{bmatrix}\sin^2\varphi, \tag{26}$$

$$\underline{\underline{r}}_{(L,R)} = \begin{bmatrix} r_C & r_{CX} \\ r_{CX} & r_C \end{bmatrix} + ir_{CX}\begin{bmatrix} 0 & -1 \\ 1 & 0 \end{bmatrix}\sin 2\varphi - \\ - 2r_{CX}\begin{bmatrix} 0 & 1 \\ 1 & 0 \end{bmatrix}\sin^2\varphi. \tag{27}$$

It is evident that the first g-o term in the CR/CL decomposition (26)–(27) takes over the role of the Fresnel matrices $\underline{\underline{t}}_{(p,s)}$ and $\underline{\underline{r}}_{(p,s)}$ in the TM/TE decomposition (13)–(14). The two next terms in Eqs. (26)–(27) are just the XPC modifications to this g-o contribution. There are significant differences between the decomposition (13)–(14) in the TM/TE basis and the decomposition (26)–(27) in the CR/CL basis. Here the first-order terms show the additional phase shift by $\pi/2$ and the second-order (antidiagonal) term is caused by the XPC effect, contrary to the case of the TM/TE case. Moreover, the

zero-order (g-o) matrices in the decomposition (26)–(27) are not diagonal. The XPC effects directly enter into the g-o beam field specification and excite the nonzero field distribution in the opposite beam component. However, this XPC contribution still does not change the beam winding number and thus does not excite new vortex.

As the g-o terms do not depend on φ, the g-o term usually dominates over the weaker higher-order terms for small values of φ. It is only one exception – normal incidence of the beams, where $t_{CX} = 0 = r_{CX}$ and the g-o matrices in Eqs. (26)–(27) become diagonal and independent of the XPC effect. That implies that, for normal incidence, optical vortices are undistorted and clearly visible in both, spectral and configuration, domains. Still it is evident that, for any beam incidence, only the first-order and second-order XPC terms in the decomposition (26)–(27) describe the vortex creation at the interface.

Potential of the relations (23)–(27) can be tested by the analysis of the ELG/PELG beams at the interface. The definition (7) is equivalent to the algebraic expression in the spectral domain:

$$\widetilde{G}_{p,l}^{(EL)}(\kappa,\overline{\kappa},Z') = (iw_w)^{2p+l}\kappa^{p+l}\overline{\kappa}^{p}\,\widetilde{G}_{0,0}^{(EL)}(\kappa,\overline{\kappa},Z'), \quad (28)$$

where $\kappa = 2^{1/2}(k_X + ik_Y) = \kappa_\perp \exp(i\varphi)$, $\overline{\kappa}$ means complex conjugate of κ, $\kappa_\perp^2 = \kappa\overline{\kappa}$, $\widetilde{G}_{p,l}^{(EL)}$ and $\widetilde{G}_{0,0}^{(EL)} = 2\pi\,\exp(-\kappa_\perp^2 v^2)$ are the Fourier transformed ELG/PELG and Gaussian beams, respectively. For incidence of the beam field $\underline{\widetilde{E}}^{(i)} = [a_R, a_L]^T\,\widetilde{G}_{p.l}^{(EL)}$ of the mode $\widetilde{G}_{p,l}^{(EL)}$ and of arbitrary polarization $\widetilde{\chi}_{(R,L)}^{(i)} = \widetilde{a}_R/\widetilde{a}_L$, specified by the in general nonuniform and complex beam components $\widetilde{a}_R$ and $\widetilde{a}_R$, the relations (23)–(24) yield:

$$\begin{bmatrix} \widetilde{E}_R^{(t)} \\ \widetilde{E}_L^{(t)} \end{bmatrix} = t_C \begin{bmatrix} \widetilde{a}_R \\ \widetilde{a}_L \end{bmatrix} \widetilde{G}_{p,l}^{(EL)} + t_{CX} \begin{bmatrix} \widetilde{a}_L \widetilde{G}_{p+1,l-2}^{(EL)} \\ \widetilde{a}_R \widetilde{G}_{p-1,l+2}^{(EL)} \end{bmatrix}, \quad (29)$$

$$\begin{bmatrix} \widetilde{E}_L^{(r)} \\ \widetilde{E}_R^{(r)} \end{bmatrix} = r_C \begin{bmatrix} \widetilde{a}_R \\ \widetilde{a}_L \end{bmatrix} \widetilde{G}_{p,l}^{(EL)} + r_{CX} \begin{bmatrix} \widetilde{a}_L\, \widetilde{G}_{p+1,l-2}^{(EL)} \\ \widetilde{a}_R\, \widetilde{G}_{p-1,l+2}^{(EL)} \end{bmatrix}, \quad (30)$$

where Eq. (28) and the identity $\kappa^{p+l}\overline{\kappa}^{p} = \kappa_\perp^{2p+l}\exp(il\varphi)$ were applied [1].

If the incident ELG beam has only *one* component of, say, CR (CL) circular polarization, the interface action yields also the ELG beam but with *two* orthogonal components. The first component has the same CR (CL) polarization as the incident beam is excited by the g-o terms in Eqs. (23)–(24) and the second component, with the opposite CL (CR) polarization, is excited by the XPC terms in these equations. Contrary to the first component, which preserves indexes of the incident beam ($p \to p$ and $l \to l$), in the second, opposite component the radial index is changed by one ($p \to p \mp 1$) and the azimuthal index is changed by 2 ($l \to l \pm 2$). So the order $N^{(EL)} = 2p + l$ of all ELG beam components remains unchanged ($N^{(EL)} \to N^{(EL)}$).

For oblique incidence the beam field definition (7) acquires the additional phase shift (1) what implies the symmetric in the $\varsigma - \overline{\varsigma}$ plane spectral shift in the definition (28):

$$\widetilde{G}_{p,l}^{(EL)}(\kappa,\overline{\kappa},Z') \to$$

$$\to \widetilde{G}_{p,l}^{(EL)}(\kappa - 2^{-1/2}k\sin\theta^{(i)}, \overline{\kappa} - 2^{-1/2}k\sin\theta^{(i)}, Z'). \quad (31)$$

The excitation problem appears now different and is affected by the narrow azimuthal range of the beam spectrum where the relations (26)–(27) are more appropriate. A position of the vortex excited by the XPC effect is shifted in this case by $-2^{-1/2}k^{(i)}\sin\theta^{(i)}$ and could be visible only when the beam spectrum range is sufficiently wide to be larger that this spectral shift. Still the relations of the global topological charge of the beams remain the same as for normal incidence. In contrast to the EHG/PEHG beam decomposition (26)–(27), the ELG/PELG decompositions (29)–(30) are exact. All terms, including the first-order and second-order terms, are accounted for in this decomposition. It is also highly symmetric. In spite of the obvious difference between C and CX coefficients the relations (29)–(30) differentiate between CR and CL polarization of the incident beam only by the changes of the indices p and l in the XPC term. Note the (constant) spectral shift (31) removed and the replacement CR $\rightleftharpoons$ CL set above the Brewster angle in Figs. 4–7.

The case of the normally incident CL polarized $\mathrm{ELG}_{2,4}$ beam collimated at the interface ($z = 0 = Z_w$) is shown in Fig. 4. The field phase distributions in the configuration and spectral domains are shown for the incident beam and for two orthogonal components of the reflected beam. All the phase distributions are circularly symmetric in the interface plane with the vortex singularity placed exactly in the centre of the figure. The beam phase change along a closed loop about this point equal to $4 \times 2\pi$ for the incident beam and for the CR component of the reflected beam. However, it equals to $2 \times 2\pi$ for the CL component of the reflected beam, as exactly predicted by Eq. (30). Excitation efficiency of this opposite beam component amounts about one order in beam intensity less than that for the direct component of the (CR) polarization. Results of numerical simulations shown in Fig. 4 for beam reflection are entirely consistent with those for beam transmission given in [1].

The case of critical incidence of the CL polarized $\mathrm{ELG}_{2,4}$ beam collimated at the interface is shown in Fig. 5 through the beam field intensity and phase distribution only in the spectral domain this time. As for the PEHG beams the symmetry specific to normal incidence is broken by (i) narrow, with respect to the paraxial limit, beam radii (ii) the oblique phase fronts of the beams in the interface plane, (iii) asymmetry of the Fresnel coefficients with respect to $\vartheta^{(i)}$ and by (iv) narrow, with respect to the beam phase shift, azimuthal range of the incident beam spectrum. For the reasons (i) and (ii) even the incident beam intensity shows deviations from the elliptic symmetry (cf. Fig. 5a) in the spectral domain. For (iii) the reflected beam spectra in both polarization components are almost annihilated for rays of $\vartheta^{(i)}$ less that the critical

angle $\theta_c^{(i)}$ (cf. Fig. 5b and Fig. 5c). Moreover, for (iv) the first-order and the second-order contributions to the reflected field are still dominated by the zero-order, g-o terms in the field decomposition (29)–(30), in spite of the fact that $r_C = 0$ exactly at $\vartheta^{(i)} = \theta_c^{(i)}$. These effects lead to severe deformations in beam amplitude and phase vivid in the configuration domain. The beam field is so badly deformed that any concise geometrical interpretation of what it really shows would be rather difficult.

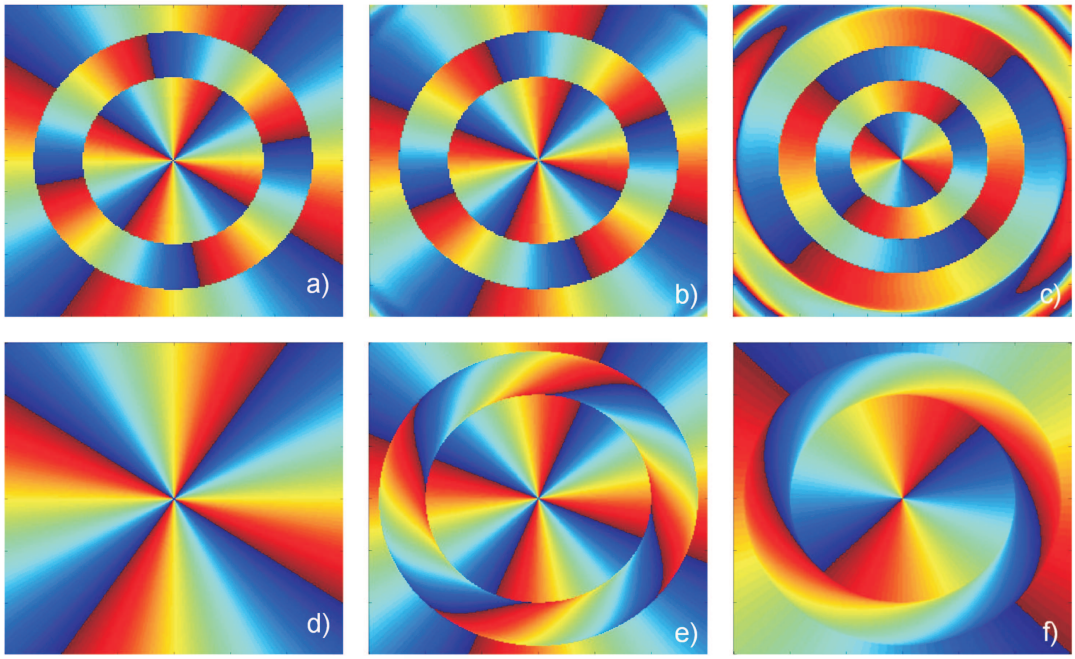

Fig. 4. Phase transverse distribution of the ELG beam components evaluated in the interface plane; counterparts of the Figs. (a)-(c) in the configuration domain are depicted in the Figs. (d)-(f) in the spectral domain, respectively. The case of normal incidence of the collimated beam is displayed for: (a) the incident beam of the $ELG_{2,4}$ pattern and of CL polarization, (b) the reflected beam CR component of the $ELG_{2,4}$ pattern, (c) the reflected beam CL component of the $ELG_{3,2}$ pattern (colour online)

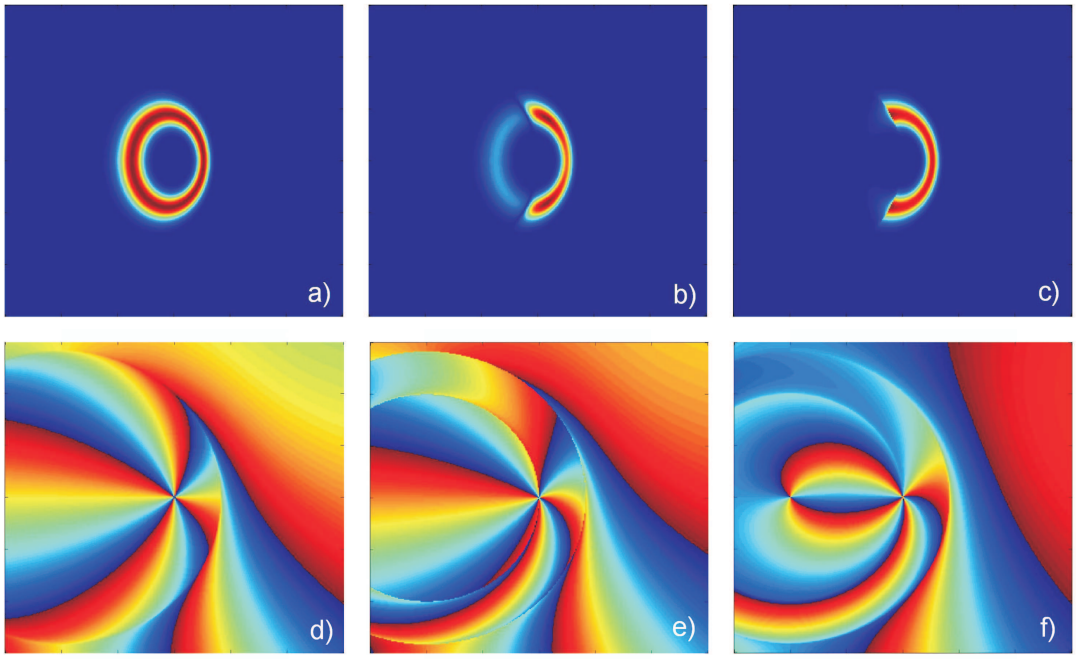

Fig. 5. Transverse field distribution of the PELG beam spectral components evaluated in the interface plane. The case of critical incidence of the collimated beam is displayed for: intensity (a) and phase (d) of the incident beam of the $PELG_{2,4}$ pattern and of CL polarization, intensity (b) and phase (e) of the reflected beam CL component of the $PELG_{2,4}$ pattern, intensity (c) and phase (f) of the reflected beam CR component of the $PELG_{3,2}$ pattern (colour online)

However, even in this case, the field distribution is still quite clear in the spectral domain because the symmetry of the beam phase structure, known from the case of normal incidence, survives here to a large extent. The on-axis vortex of the topological charge equal to 4 is placed exactly in the central ray position of the beam (for $\vartheta = \theta_c^{(i)}$ or $k_X w_w = k^{(i)} w_w \sin\theta^{(i)}$) for the incident beam (cf. Fig. 5d), as well as for the reflected beam components of the direct CL polarization (cf. Fig. 5e). Moreover, the vortex of same type can be spotted in the spectrum of the opposite (CR) component (cf. Fig. 5f). Still the global topological charge of the excited vortices equals to 2 as expected, because the second, off-axis vortex of the opposite charge equal to -2 is also excited at $k_X w_w = 0$ (cf. Fig. 5f). The spectral position of this additional vortex is displaced by $-k^{(i)} w_w \sin\theta^{(i)}$ to the point $k_X w_w = 0$, that is where $r_{CX} = 0$. A trace of this vortex is weak and difficult to observe in points where the spectral intensity is low for not sufficiently narrow beams. Note that in all figures the beam spectrum is shown as displaced by $-k^{(i)} w_w \sin\theta^{(i)}$ to have $k_X w_w = 0$ at the beam spectrum centre.

Numerical results presented in Fig. 5 not only confirm predictions of Eqs. (19)–(30) but also directly explain the mechanism of vortex creation or annihilation caused by the XPC effect at the interface. The change by 2 of the topological charge in the opposite beam component, as predicted by Eqs (19)–(30), results from creation of the additional, off-axis in general, vortex of the topological charge equal to plus or minus 2. The topological charge of this additional vortex adds to or subtracts from the topological charge of the vortex which mimics that of the incident beam. That suggests that the angular momentum conservation principle [24–26], valid for normal incidence of the ELG beams [1], may also remain valid for PELG beams under oblique incidence.

The process depends directly on the relative sign of the phase rotation, indicated by the signs of the azimuthal index l, with respect to the sign of rotation of the field vector, distinguished by the beam CR or CL polarization (cf. Fig. 6). The process depends also on the beam waist position or, alternatively, on the beam propagation. Figure 7 displays, for different positions of the beam waist centre above the interface, helical rotations of the reflected beam phase structure about its vortex singularities. The beam phase structure rotates about the field phase singularities with the vortex centres remained robust with no displacements of their spectral positions.

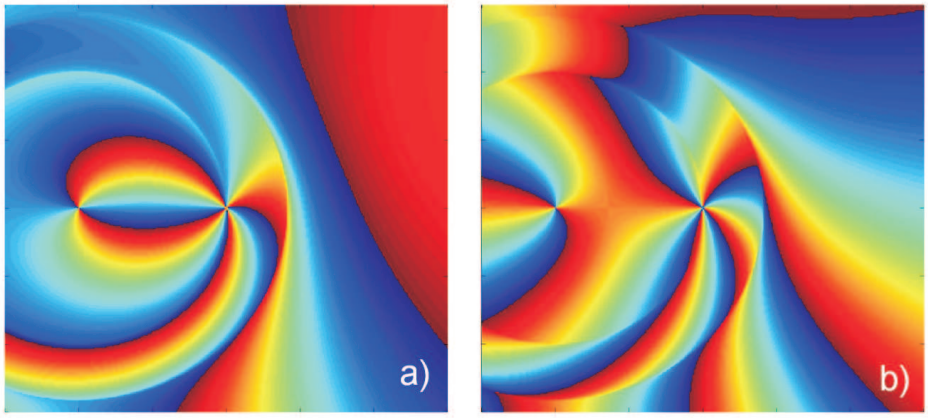

Fig. 6. Optical vortex excitation and splitting induced by the XPC effect for the incident beam of the $\mathrm{ELG}_{2,4}$ shape. Phase distribution of the reflected beam at the interface (a) for *CL polarization* of the incident beam and *CR polarization* of the reflected beam component with the total topological charge equal to $4-2$, (b) for *CR polarization* of the incident beam and *CL polarization* of the reflected beam component with the total topological charge equal to $4+2$. Dependence of the vortex excitation and splitting phenomena on incident beam polarization is shown by differences between Figs. (a) and (b). All other data are the same as for Fig. 5 (colour online)

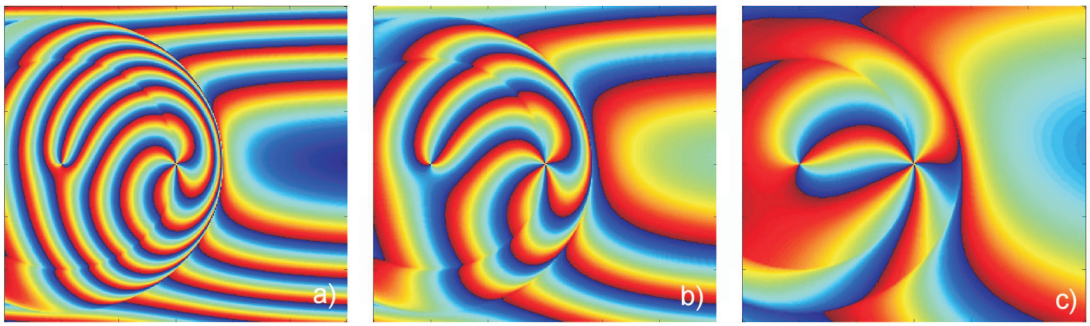

Fig. 7. Vortex phase evolution of the reflected *CR polarized* beam of the $\mathrm{ELG}_{3,2}$ shape shown in the spectral domain in the interface plane for different incident beam waist positions placed at: $z/z_D =$: (a) -1.0, (b) -0.5, (c) -0.125. The case of $z/z_D = 0.0$ is shown in Fig. 5f and 6a. All other data are the same as for Fig. 5 (colour online)

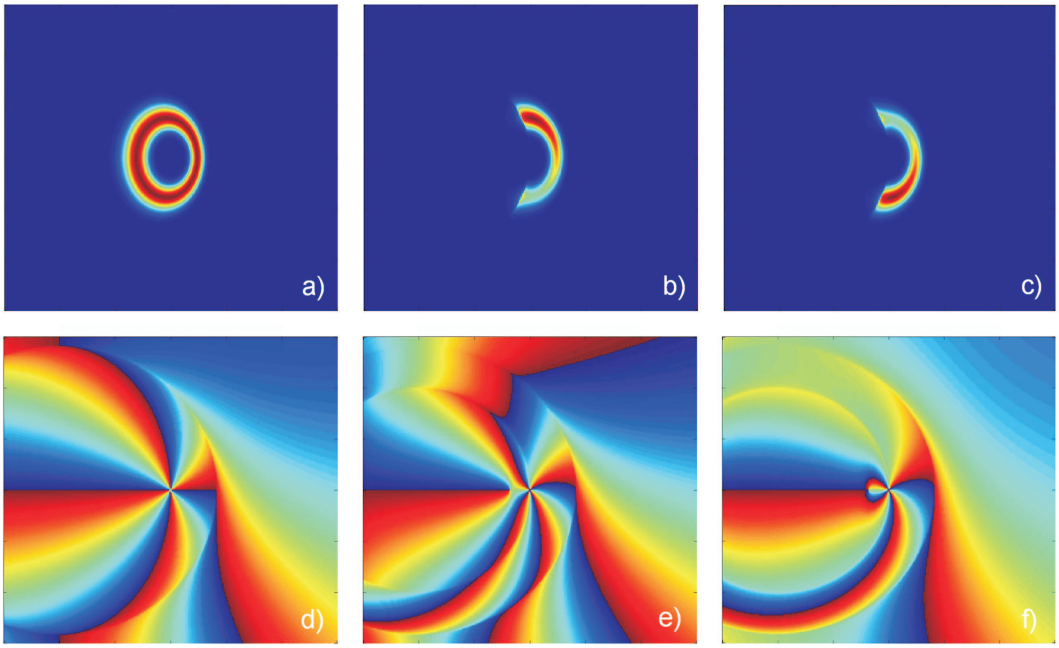

Fig. 8. Transverse distribution of the common elegant LG beam spectral components evaluated in the interface plane. The case of critical incidence of the elliptic beam is displayed for: intensity (a) and phase (d) of the incident beam of the *common* $ELG_{2,4}$ *pattern* and of CL polarization, intensity (b) and phase (e) of the reflected beam CL component pattern, intensity (c) and phase (f) of the reflected beam CR component pattern. All other data are the same as for Fig. 5, where the reflection was presented for the *projected elegant beam* $PELG_{2,4}$ (colour online)

Still, the issue to what extend the patterns of the *commonly* defined elegant beams, i.e. those of the elegant beams defined in their transverse $x-y$ (waist) planes, follow the *projected* elegant beam patterns, i.e. those of the elegant beams defined in the interface $X-Y$ plane, remains open. In principle, this issue can be elucidated by determination of the expansion coefficients of the beam field representation (1). However, some view of the problem can be also directly obtained by comparison of the common and projected beam patterns simulated numerically. For EHG and PEHG beams the differences do not seem to be qualitative (cf. Fig. 2 in [18]), contrary to the case of the elliptic ELG and PELG beam reflection, as it is evident from their critical incidence presented in Fig. 8.

For oblique incidence of the common ELG beam an average spectral intensity of the reflected beam is displaced transversally from the beam centre position in the $\pm Y$ direction depending on the sense (CR or CL) of beam polarization. At the same time the displacement of the excited by the XPC effect vortex position is degenerated much with respect to the case of the pure PELG beam incidence presented in Fig. 5. Moreover, some trace of the vortex splitting can also be found in the second reflected beam component. Therefore, in the case of the standard ELG beam incidence, the spectral vortex splitting is attributed to both orthogonal beam components of CR and CL polarization. All of that indicates that the standard ELG beam should be represented by more than one element of the expansion (1) and that, contrary to the projected elegant beams, the common elegant beams cannot be considered as normal modes of the interface in the case of beam oblique incidence.

Figures 4–8 visualise the main result of the paper – the description of the vortex excitation phenomenon at the interface in its spectral aspects. The figures show explicitly its dependence on beam incidence and indicate positions of the excited vortices precisely at points obtained entirely by the theoretical analysis presented. The process depends on the range of beam spectrum and become efficient when this range covers points of vortex centre positions, that is in cases of narrow non-paraxial beams. It always happens for normal incidence. For oblique incidence it depends on the balance between beam incidence and beam width – when the incidence angle becomes larger, the beam width should become smaller. Characteristic features of the beam transmission, especially those dependent on beam incidence angle and spectrum range, have been also examined in [22] for arbitrary values of the polar incidence angle. It seems that the phenomena of vortex excitation and splitting are characteristic for interactions of non-paraxial beams with the interface. Their origin is the XPC effect at the interface.

5. Summary and conclusions

Main aspects of the beam-interface interactions have been analysed theoretically and numerically on the grounds on the rigorous vector theory of beam fields at the interface [1]. For normal incidence the elegant HG and LG beams are considered with their possible extension into the non-paraxial range. For oblique incidence the common elegant beams are replaced by their projections PHG and LHG beams suitable for the beam field analysis in terms of a vector normal mode expan-

sion at the interface. All theoretical expressions given here are quite general and in addition all of them are exact in the circular polarization basis projected upon the interface plane. They cover all cases of internal and external reflection and refraction, with normal and oblique incidence and possibly with direct extension to the case of grazing incidence [27]. In the analysis special care has been paid for phenomena of coupling existed between the beam field polarization and the beam field distribution in its amplitude and phase, as originated by the cross-polarization coupling at the interface [1, 15–18].

It was shown that the Fresnel transmission/reflection coefficients should be replaced by their generalisations appropriate for 3D beams of finite cross-sections. All, the g-o or zero-order, first-order and second-order, contributions to the beam field are governed by new coefficients - t_C, r_C of the g-o type (25) and t_{CX}, r_{CX} of the XPC type (15). They are composed of sums and differences of the common p and s Fresnel coefficients and satisfy only two scalar field continuity relations at the interface: $t_C - 1 = -r_C$ and $t_{CX} = -r_{CX}$, in opposition to four scalar relations necessary for the Fresnel coefficients. The definitions of the coefficients t_C, r_C, t_{CX} and r_{CX} as well as the transmission/reflection matrices are quite general. They are valid not only for the dielectric interface but also for any planar multilayered structure, which is homogeneous and isotropic in any $X - Y$ plane [28].

The XPC effects exist as the non-g-o contribution to the beam field. As far as a single central ray of the beam is considered, $r_{CX} = 0 = t_{CX}$ and the XPC effects disappear for normal incidence. For critical incidence $r_{CX} = 1 = -t_{CX}$ and the g-o effects disappear in this case. The XPC effects lead to creation of higher-order or lower-order modes in the opposite – to the polarization state of the incident beam – field component and can be explicitly described by changes of the beam mode indices. Meanwhile in the rectangular coordinates these changes can be described analytically only within the first-order approximation to the field, the same analysis applied in the cylindrical coordinates appears analytically exact with no approximations needed. Still, in any case, the approximations inherent to the g-o optics [29] were omitted within this analysis.

Two sets of elegant higher-order beams, with specified further modifications, have been considered as normal modes at the interface: EHG beams of linear polarization and ELG beams with circular polarization. As the interface couples polarization and spatial (in amplitude and phase) structures of the beams, normal modes have been treated as scalar modes dressed by linear polarization for EHG modes and circular polarization for ELG modes. Both of them have been analysed for their normal incidence; for oblique incidence their PEHG and PELG projections on the interface plane have been considered instead. Only the cases of normal and critical incidence of non-paraxial beams are analysed numerically, other, paraxial cases were discussed elsewhere [18, 22].

In general, the elegant beams acquire changes in both their mode indices. However, for oblique incidence of the PEHG beam, the longitudinal index change gradually diminishes with increasing the incidence angle and is replaced by the net longitudinal spatial displacement of the whole field structure [18]. On the other hand, the ELG/PELG beams show different behaviour indicating vortex excitation in the first place. For oblique incidence the analysis reveals also vortex splitting, where a topological charge of the new vortex is opposite in sign to the charge of the vortex driven by the incident beam. To the author's knowledge it is the first theoretical derivation and its numerical verification of optical vortex splitting at the interface.

Spectral positions of these new vortices are displaced in the plane $k_Y = 0$ from the incident vortex placement at $k_X = k \sin \theta^{(i)}$ to the new position at $k_X = 0$ where the beam field is zero, due to zeroes of the XPC coefficients $t_{CX} = -r_{CX} = 0$ at this point. Therefore, meanwhile the propagation direction of the vortex nested in the incident beam coincides with the beam axis, the propagation direction of the excited vortex appears normal to the interface. The vortex excitation is efficient for non-paraxial beams where the range of beam spectra covers spectral positions of the excited vortices. The topological charge of the excited vortices equals ± 2. For both, CL and CR, polarization states of the incident LG beam, changes of spin angular momentum related to the opposite polarization of the excited beam component are compensated by changes of orbital angular momentum related to the vortices embedded in this component.

The beam field spectral distribution in amplitude and phase is here rigorously treated analytically and numerically for normal and oblique beam incidence. The numerical method applied in the numerical simulations is based on direct integration of Maxwell equations [18] and was additionally verified by independent simulations [22], for a change based directly on the equations derived in [1]. In this paper only the case of beam reflection has been numerically analysed. Numerical treatment of beam transmission, complementary to what is already available in [1], was also reported in [22]. The simulations entirely confirmed analytical predictions. Moreover, they also show that at the interface plane the field distributions of the PEHG and PELG modes defined here and of the commonly defined elegant modes [13] coincide qualitatively well when their beam waist centres are placed in the interface plane. Certainly, they coincide exactly for normal incidence.

Appendix 1

Generalised coefficients of transmission and reflection

By introduction of complex parameters of beam polarization the transmission and reflection matrices can be represented in their diagonal form, with diagonal elements given by the generalized transmission and reflection coefficients [1], specific to any planar layered structure. Their form is particularly suitable in deriving the extended Stokes reciprocity relations for beam vector modes at such the structures [28]. Definitions of these coefficients are listed below. Their relations to the diagonal transmission and reflection matrices were described in an electronic extended version of this paper [30].

By introduction the complex parameter $\widetilde{\chi}^{(i)}_{(X,Y)} = \widetilde{E}^{(i)}_X / \widetilde{E}^{(i)}_Y$ in the TM/TE matrix decomposition (13)–(14), one obtains:

$$\eta t_{TM} = \eta t_p + \Delta_{TM}, \qquad t_{TE} = t_s + \Delta_{TE}, \tag{A1}$$

$$r_{TM} = r_p - \Delta_{TM}, \qquad r_{TE} = r_s + \Delta_{TE}, \tag{A2}$$

$$\begin{aligned} \Delta_{TM} &= 2t_{CX} s_\varphi \left[{\widetilde{\chi}^{(i)}_{(X,Y)}}^{-1} c_\varphi - s_\varphi \right], \\ \Delta_{TE} &= 2t_{CX} s_\varphi \left[{\widetilde{\chi}^{(i)}_{(X,Y)}}^{+1} c_\varphi + s_\varphi \right], \end{aligned} \tag{A3}$$

where $t_{CX} = \frac{1}{2}(\eta t_p - t_s) = -r_{CX}$, $s_\varphi \equiv \sin\varphi$ and $c_\varphi \equiv \cos\varphi$. Per analogy, by the introduction the new, "circular" complex parameter $\widetilde{\chi}^{(i)}_{(R,L)} = \widetilde{E}^{(i)}_R / \widetilde{E}^{(i)}_L$ in the CR/CL matrix decomposition (23)–(24), one can also obtain the new "circular" coefficients:

$$t_{CR} = t_C + \Delta_{CR}, \qquad t_{CL} = t_C + \Delta_{CL}, \tag{A4}$$

$$r_{CR} = r_C - \Delta_{CR}, \qquad r_{CL} = r_C - \Delta_{CL}, \tag{A5}$$

$$\begin{aligned} \Delta_{CR} &= t_{CX} {\widetilde{\chi}^{(i)}_{(R,L)}}^{-1} \exp(-2i\varphi), \\ \Delta_{CL} &= t_{CX} {\widetilde{\chi}^{(i)}_{(R,L)}}^{+1} \exp(+2i\varphi), \end{aligned} \tag{A6}$$

where $t_C = \frac{1}{2}(\eta t_p + t_s) = 1 - r_C$.

In opposition to the standard Fresnel coefficients ηt_p, t_s, r_p, r_s the new, generalised coefficients ηt_{TM}, t_{TE}, r_{TM} and r_{TE} of the linear type as well as t_{CR}, t_{CL}, r_{CR} and r_{CL} of the circular type depend not only on the polar angle θ but also on the azimuthal angle φ. Although the generalized coefficients ηt_{TM}, t_{TE}, r_{TM} and r_{TE} resolve into the Fresnel coefficients ηt_p, t_s, r_p, r_s for $\varphi = 0$, these Fresnel coefficients should be replaced by their 3D generalisations (A1)–(A3) for $\varphi \neq 0$. Similarly, in the "circular" basis the matrices $\underline{\underline{t}}_{(R,L)}$ and $\underline{\underline{r}}_{(L,R)}$ become symmetric only for $\varphi = 0$ (cf. Eqs. (26)–(27)):

$$\underline{\underline{t}}_{(R,L)} = \begin{bmatrix} t_C & t_{CX} \\ t_{CX} & t_C \end{bmatrix}, \tag{A7}$$

$$\underline{\underline{r}}_{(L,R)} = \begin{bmatrix} r_C & r_{CX} \\ r_{CX} & r_C \end{bmatrix}, \tag{A8}$$

otherwise (A4)–(A6) apply. This dependence on φ of the generalized coefficients influences significantly over the 3D field distribution of the reflected and transmitted beams. Still, through logarithmic differentiation of these coefficients one can described, for example, various nonspecular phenomena of beam transmission and reflection [4, 14–16].

Appendix 2

A note on the beam shifts

A role of beam propagation and their interaction with the interface in signal enhancement techniques has been discussed recently in the context of experiments in classical and quantum optics [31]. The same concerns recent measurements within near field optics [23] and those involving surface plasmon resonances [32] or microcavities [33]. In that type of measurements the role of longitudinal and transverse beam shifts, like the lateral, angular, focal and composite beam displacements, evaluated in three dimensions [14–16], seem already essential. Note that the definitions of these displacements have been generalized from their counterparts derived within 2D geometries [34, 35], where, however, such 3D phenomena like XPC effects, I-F shifts, vortex excitations or beams of the LG type cannot be treated at all.

The problem of beam-field angular-momentum conservation at the interface has been also recently under interesting discussion, although without avoiding some controversies [36, 37]. The analyses based on geometrical optics have been carried out, within which the conservation of angular momentum at the interface was derived. The results were interpreted in terms of beam shifts of the first-order and compared with their evaluation presented previously within different approaches in [14] and [38]. However differences between results of various approaches to the problem of the beam shifts are dependent on the ratio of the beam radius to the field wavelength and become more vivid close to the paraxial limit, i.e. around $kw_w \cong 20\pi$ or less. As this issue was not raised in that discussion, it seems that the question of differences between different definitions of the beam shifts still remains open.

Moreover, averaging of the field intensity, in evaluation for example of the first-order shifts of a beam gravity centre of the beam [39], disregards its phase distribution and smears out local properties of its amplitude. In any case, for oblique incidence of narrow beams with helical structure, especially for critical incidence of TIR, the field amplitude and phase spatial distribution of the beam is so strongly deformed [9] that the direct application of the spatial shift analysis seems to be too approximate in this case. Therefore, notions of the beam spatial shifts, approximations of the g-o type or averaging procedures in the beam field evaluation are absent in the analysis presented in this paper.

In spite of that, the non-specular displacements like HG and IF shifts still might serve well as the additional geometrical interpretation of the HG beam field distribution obtained otherwise by a more accurate method [18]. It seems that these displacements can also be used in the treatment of the LG beams, for example with the help of diagonal relations between the HG and LG beams [24, 25]. Definitions of these displacements, or more precisely the longitudinal and transverse beam translations, angular deviations and coordinate scaling [14–16], are evaluated up to the second-order level, do not need any field averaging in their evaluation, avoid simplifications commonly encountered in energy-flux methods [39] and are free from adiabatic approximations inherent to g-o analyses [29]. They are valid for beam refraction and reflection under arbitrary incidence at any planar, layered structure [28] and may yield good although approximate interpretation of the paraxial beam field distributions at the interface.

REFERENCES

[1] W. Nasalski, "Polarization versus spatial characteristics of optical beams at a planar isotropic interface", *Phys. Rev.* E 74, 056613-1-16 (2006).

[2] M. Born and E. Wolf, *Principles of Optic*s, Cambridge University Press, Cambridge, 1999.

[3] P. Yeh, *Optical Waves in Layered Media,* Wiley, New York, 1976.

[4] W. Nasalski, "Optical beams at dielectric interfaces – fundamentals", in Series: *Trends in Mechanics of Materials*, IPPT PAN, Warsaw, 2007.

[5] J. Picht, "Beitrag zur Theorie der Totalreflexion", *Ann. Phys. Leipzig* 5, 433–496 (1929).

[6] F. Goos and H. Hänchen, "Ein neuer and fundamentaler Versuch zur Totalreflexion", *Ann. Phys. Leipzig* 1, 333–345 (1947).

[7] F.I. Fedorov, "K teorii polnovo otrazenija", in: *Dokl. Akad. Nauk SSSR* 105, 465–467 (1955), (in Russian).

[8] C. Imbert, "Calculation and experimental proof of the transverse shift induced by total internal reflection of a circularly polarized light beam", *Phys. Rev*. D 5, 787–796 (1972).

[9] H. Okuda and H. Sasada, "Significant deformations and propagation of Laguerre-Gaussian beams reflected and transmitted at a dielectric interface", *J. Opt. Soc. Am.* A 25, 881–890 (2008).

[10] R. Zambrini and S. M. Barnett, "Quasi-intrinsic angular momentum and the measurement of its spectrum", *Phys. Rev. Lett.* 96, 13901-1-4 (2006).

[11] G. Molina-Terriza, J.P. Torres, and L. Torner, "Management of the angular momentum of light: preparation of photons in multidimensional vector states of angular momentum", *Phys. Rev. Lett.* 88, 013601-1-4 (2002).

[12] A.E. Siegman, "Hermite-Gaussian functions of complex argument as optical beam eigenfunctions", *J. Opt. Soc. Am*. 63, 1093–1995 (1973).

[13] A.E. Siegman, *Lasers*, University Science Books, Mill Valley, 1986.

[14] W. Nasalski, "Longitudinal and transverse effects of nonspecular reflection", *J. Opt. Soc. Am.* A 13, 172–181 (1996).

[15] W. Nasalski, "Three-dimensional beam reflection at dielectric interfaces", *Opt. Commun*. 197, 217–233 (2001).

[16] W. Nasalski, "Amplitude-polarization representation of three-dimensional beams at a dielectric interface", *J. Opt. A: Pure Appl. Opt*. 5, 128–136 (2003).

[17] A. Köházi-Kis, "Cross-polarization effects of light beams at interfaces of isotropic media", *Opt. Commun*. 253, 28–37 (2005).

[18] W. Nasalski and Y. Pagani, "Excitation and cancellation of higher-order beam modes at isotropic interfaces", *J. Opt. A: Pure Appl. Opt.* 8, 21–29 (2006).

[19] S. Saghafi and C.J.R. Sheppard, "Near field and far field of elegant Hermite-Gaussian and Laguerre-Gaussian modes", *J. Mod. Opt.* 45, 1999–2009 (1998).

[20] J. Enderlein and F. Pampaloni, "Unified operator approach for deriving Hermite-Gaussian and Laguerre-Gaussian laser modes", *J. Opt. Soc. Am*. A 21, 1553–1558 (2004).

[21] A. April, "Nonparaxial TM and TE beams in free space", *Opt. Lett*. 14, 1563–1565 (2008).

[22] W. Szabelak and W. Nasalski, „Transmission of Elegant Laguerre-Gaussian beams at a dielectric interface – numerical simulations", *Bull. Pol. Ac.: Tech*. 57, 181–188 (2009).

[23] F.I. Baida, D. Van Labeke, J-M. Vigoureux, "Numerical study of the displacement of a three-dimensional Gaussian beam transmitted at total internal reflection. Near-field applications", *J. Opt. Soc. Am.* A 17, 858–865 (2000).

[24] L. Allen, M.W. Beijersbergen, R.J.C. Spreeuw, and J.P. Woerdman, "Orbital angular momentum of light and the transformation of Laguerre-Gaussian laser modes", *Phys. Rev.* A 45, 8185–8189 (1992).

[25] L. Allen, M.J. Padgett, and M. Babiker, "The orbital angular momentum of light", *Progress in Optics* 39, 291–372 (1999).

[26] A.T. O'Neil, I. Mac Vicar, L. Allen, and M.J. Padgett, "Intrinsic and extrinsic nature of the orbital angular momentum of a light beam", *Phys. Rev. Lett.* 88, 053601-1-4 (2002).

[27] C.K. Carniglia and L. Mandel, "Quantization of evanescent electromagnetic waves", *Phys. Rev.* D 3, 280–296 (1971).

[28] W. Nasalski, "Three-dimensional beam scattering at multilayers: formulation of the problem", *J. Tech. Phys.* 45, 121–139 (2004).

[29] G.A. Deschamps, "Ray techniques in electromagnetics", *Proc. IEEE* 60, 1022–1035 (1972).

[30] W. Nasalski, "Elegant vector normal modes at a dielectric interface", arXiv: 0810.2291, 1–28 (2008).

[31] A. Aiello and J.P. Woerdman, "Role of beam propagation in Goos-Hänchen and Imbert-Fedorov shifts", *Opt. Lett.* 33, 1437–1439 (2008).

[32] X. Yin, L. Hesselink, H. Chin, and D.A.B. Miller, "Temporal and spectral nonspecularities in reflection at surface plasmon resonance", *Appl. Phys. Lett*. 89, 041102-1-3 (2006).

[33] D.H. Foster, A.K. Cook, and J.U. Nöckel, "Goos-Hänchen induced vector eigenmodes in a dome cavity", *Opt. Lett.* 32, 1764–1766 (2007).

[34] T. Tamir, "Nonspecular phenomena in beam fields reflected by multilayered media", *J. Opt. Soc. Am.* A 3, 558–565 (1986).

[35] W. Nasalski, T. Tamir, and L. Lin, „Displacement of the intensity peak in narrow beams reflected at a dielectric interface", *J. Opt. Soc. Am*. A 5, 132–140 (1988).

[36] M. Onoda, S. Murakami, and N. Nagaosa, "Geometrical aspects in optical wave-packet dynamics", *Phys. Rev.* E 74, 066610-1-29 (2006).

[37] K. Yu. Bliokh and Yu.P. Bliokh, "Polarization, transverse shifts, and angular momentum conservation laws in partial reflection and refraction of an electromagnetic wave packet", *Phys. Rev.* E 75, 066609-1-10 (2007).

[38] V.G. Fedoseyev, "Spin-independent transverse shift of the centre of gravity of a reflected and of a refracted light beam", *Opt. Commun.* 193, 9–18 (2001).

[39] K. Yasumoto and Y. Oishi, "A new evaluation of the Goos-Hänchen shift and associated time delay", *J. Appl. Phys.* 54, 2170–2176 (1983).